Biotechnol Lett (2017) 39:1245–1252
DOI 10.1007/s10529-017-2358-6

ORIGINAL RESEARCH PAPER

Peroxide-dependent oxidation reactions catalyzed by CYP191A1 from *Mycobacterium smegmatis*

Hye-Yeong Jo · Sun-Ha Park · Thien-Kim Le · Sang Hoon Ma · Donghak Kim · Taeho Ahn · Young Hee Joung · Chul-Ho Yun

Received: 14 March 2017 / Accepted: 9 May 2017 / Published online: 19 May 2017

Abstract
Objectives To find the catalytic activities of CYP191A1 from *Mycobacterium smegmatis*, in which functions of most P450s are unknown, by using a set of reductase systems, peroxides, and various substrates including fatty acids and human drugs.
Results CYP191A1 was functionally expressed in *Escherichia coli* and purified. Its catalytic activities were examined with fatty acids, chromogenic and fluorogenic substrates, and several human P450 substrates, in the presence of six different types of electron transfer systems, such as rat NADPH-P450 reductase, *Candida* NADPH-P450 reductase, ferredoxin/ferredoxin reductase, putidaredoxin/putidaredoxin reductase, and peroxides (H_2O_2 and *t*-butyl hydroperoxide). The reactions catalyzed by CYP191A1 included the hydroxylation and *O*-dealkylation of several substrates.
Conclusions CYP191A1 preferentially catalyzes the peroxide-dependent oxidation of various substrates over the reductase-dependent reaction. Its peroxygenase activity may be used an effective biocatalytic tool to synthesize the metabolites of drugs.

Keywords CYP191A1 · Cytochrome P450 · Fatty acid · Human P450 substrate · Peroxide · Peroxygenase activity

Electronic supplementary material The online version of this article (doi:10.1007/s10529-017-2358-6) contains supplementary material, which is available to authorized users.

Hye-Yeong Jo and Sun-Ha Park have contributed equally to this work.

H.-Y. Jo · S.-H. Park · T.-K. Le · S. H. Ma · Y. H. Joung · C.-H. Yun (✉)
School of Biological Sciences and Technology, Chonnam National University, 77 Yongbongro, Gwangju 61186, Republic of Korea
e-mail: chyun@jnu.ac.kr

D. Kim
Department of Biological Sciences, Konkuk University, Seoul 05029, Republic of Korea

T. Ahn
College of Veterinary Medicine, Chonnam National University, Gwangju 61186, Republic of Korea

Introduction

Because *Mycobacterium smegmatis* is similar to pathogenic species of *Mycobacterium*, such as those that cause tuberculosis (*Mycobacterium tuberculosis*) and leprosy (*Mycobacterium leprosy*), it is considered as a model system to investigate the pathological process of harmful mycobacteria (Guardiola-Diaz et al. 2001). In particular, *M. tuberculosis* contains 20 genes encoding cytochromes P450 (P450), which have been extensively studied as drug targets for tuberculosis (Ouellet et al. 2010). A genome analysis of *M. smegmatis* indicates that this species contains 40

putative P450 enzymes (http://drnelson.uthsc.edu/CytochromeP450.html). To date, the functions of only six P450 genes of *M. smegmatis* have been reported: CYP125A3 (García-Fernández et al. 2013), CYP142A2 (García-Fernández et al. 2013) CYP125A4 (Frank et al. 2015), CYP164A2 (Warrilow et al. 2009), CYP51 (Jackson et al. 2003), and CYP151A1 (Poupin et al. 1999). The lack of information regarding the natural redox partners, such as ferredoxin/ferredoxin reductase (FDR/Fdx), for the corresponding P450s limits the study of the natural functions of the P450s in *M. smegmatis.*

In this study, we examined the catalytic activities of CYP191A1 from *M. smegmatis*, an orphan P450 assigned to the P450 superfamily but without a known cellular or biochemical function, using a set of reductase systems and peroxides. H_2O_2 and *t*-butyl hydroperoxide (*t*-BHP). The substrates tested were fatty acids, chromogenic and fluorogenic substrates, and human drug substrates (Supplementary Fig. 1). A second goal of this study was to examine possible candidates for redox partners that can transfer electrons to CYP191A1 using various reductase enzymes. Need of electron transfer from nicotinamide adenine dinucleotide (phosphate) (NAD(P)H) via proper redox partner proteins for the P450 catalysis limits a broader technical implementation of P450 enzymes (Bernhardt and Urlacher 2014). The reductase systems tested here were rat NADPH-P450 reductase (rCPR), Candida CPR (CaCPR), FDR/Fdx, putidaredoxin reductase/putidaredoxin (PDR/Pdx), and peroxides such as H_2O_2 and *t*-BHP. Here, we showed that CYP191A1 can act as a P450 peroxygenase that bypasses the general P450 reaction mechanism. Thus, this peroxygenase activity of CYP191A1 can be used as a biocatalyst to generate hydroxylated fatty acids and human drug metabolites.

Materials and methods

Materials

Mycobacterium smegmatis mc^2 155 (ex Korean Collection for Type cultures) was used

N,O-Bis(trimethylsilyl)trifluoroacetamide (BSTFA), H_2O_2, *t*-BHP, spinach Fdx, spinach FDR, and IPTG, capric acid, lauric acid, myristic acid, palmitic acid. 7-ethoxycoumarin (7-EC), 7-ethoxy-4-trifluoromethylcoumarin (7-EFC), 7-methoxyresorufin and 7-pentoxyresorufin, chlorzoxazone, simvastatin, lovastatin, resveratrol, chlorzoxazone, atorvastatin, and phenacetin were obtained from Sigma-Aldrich.

Spectral binding titrations

Spectral binding titrations were performed to determine the dissociation constants (K_s) for the substrates. The binding affinities of the substrates to CYP191A1 were determined by titrating 1 μM enzyme with each ligand (substrate) in 1 ml 100 mM potassium phosphate buffer (pH 7.4). The reference cuvette, which contained an equal concentration of enzyme in buffer, was titrated with an equal volume of the solvent. Spectra (350–500 nm) were recorded after each addition of substrate, and the absorbance differences were plotted against the concentration of the added ligand. The spectral dissociation constants (K_s) were estimated using One site binding (hyperbola) equation (GraphPad Software, San Diego, CA): $\Delta A = B_{max} \cdot S/(K_s + S)$, where S represents substrate concentration, K_s is the spectral dissociation constant, and B_{max} is the maximal binding.

CYP191A1 catalytic activity assays

The catalytic activities of CYP191A1 were studied using several types of substrates, including fatty acids, chromogenic and fluorogenic substrates, and drug substrates (Supplementary Fig. 1). Six electron transport systems were used to compare the CYP191A1-catalyzed reactions: rCPR, CaCPR, FDR/Fdx, PDR/Pdx, H_2O_2, and *t*-BHP at 100 μM rCPR, 100 μM CaCPR, 0.1 units of FDR/22 μg of Fdx, or 50 pmol of PDR/250 pmol of Pdx in 0.25 ml of 100 mM potassium phosphate buffer (pH 7.4). The reaction mixture consisted of 0.4 μM of CYP191A1, an electron transport system and a specified amount of the substrates in 0.25 ml of 100 mM potassium phosphate buffer (pH 7.4). After preincubation for 5 min at 37 °C, an aliquot of an NADPH-generating system for rCPR, CaCPR and FDR/Fdx or 1 mM NADH for PDR/Pdx was used to initiate the reactions; the final concentrations of the NADPH–generating system were 10 mM glucose-6-phosphate, 0.5 mM $NADP^+$, and 1.0 IU glucose 6–phosphate dehydrogenase/ml. The reactions were usually performed for 5 min at 37 °C.

The reactions supported by peroxide included 0.8 μM CYP191A1 in 0.5 ml 100 mM potassium phosphate buffer (pH 7.4) along with a specified amount of the substrates. After a preincubation for 5 min at 37 °C, an aliquot of H_2O_2 or *t*-BHP (10 mM) was used to initiate the reactions. The reactions were performed for 5 min at 37 °C.

Results and discussion

Heterologous expression of *M. smegmatis* CYP191A1 in *Escherichia coli*

The CYP191A1 gene from *M. smegmatis* is 1,215 bp in length and encodes a protein of 416 amino acids and with a molecular mass of 46 kDa (Fig. 1b, Supplementary Fig. 2). Although only four CYP genes from genus *Mycobacterium* classified as CYP191A subfamily have been reported, their catalytic activities are unknown. When the amino acid sequence of CYP 191A1 was compared to that of 191A2, 191A3, and 191A4, the identities of 191A1 to the corresponding CYP191A proteins were 69, 70, and 78%, respectively (Supplementary Fig. 2).

Spectral properties of the purified CYP191A1 enzyme

The absolute spectra were determined for the oxidized form, the dithionite-reduced form, and the reduced carbon monoxide form of the enzyme. The ferric form of purified CYP191A1 was mainly in the low-spin state with a Soret band at 420 nm, whereas the ferrous form of the protein resulted in a broad absorption peak at approximately 420 nm (Fig. 1a). The high-spin iron fraction of the CYP191A1 was estimated from a second-derivative analysis of the absorption spectra. The low-spin state was dominant in the CYP191A1 sample (65% low-spin).

Spectral equilibrium binding titrations of purified CYP191A1 enzyme for substrates

The binding titration of the fatty acids tested here with CYP191A1 resulted in a type I shift in the heme Soret band, with an increase in the absorbance at 390 nm and a decrease in the absorbance at 420 nm (Fig. 2). This result is indicative of the removal of H_2O as the sixth ligand of the heme iron and the conversion from the low- to the high-spin form. The binding affinities of CYP191A1 toward the fatty acids capric acid (C_{10}) ($K_s = 545 \pm 49$ μM), lauric acid (C_{12}) ($K_s = 44 \pm 4$ μM), myristic acid (C_{14}) ($K_s = 8.9 \pm 1.3$ μM), and palmitic acid (C_{16}) ($K_s = 5.3 \pm 0.5$ μM) were determined. CYP191A1 they exhibited affinity as $C_{16} > C_{14} > C_{12} > C_{10}$.

When 4-NP, 7-EC, 7-EFC, chlorzoxazone, simvastatin, and lovastatin were added to the CYP191A1, apparent spectral changes were not observed; thus the dissociation constants could not be determined. This result suggests that the binding of these chemicals to

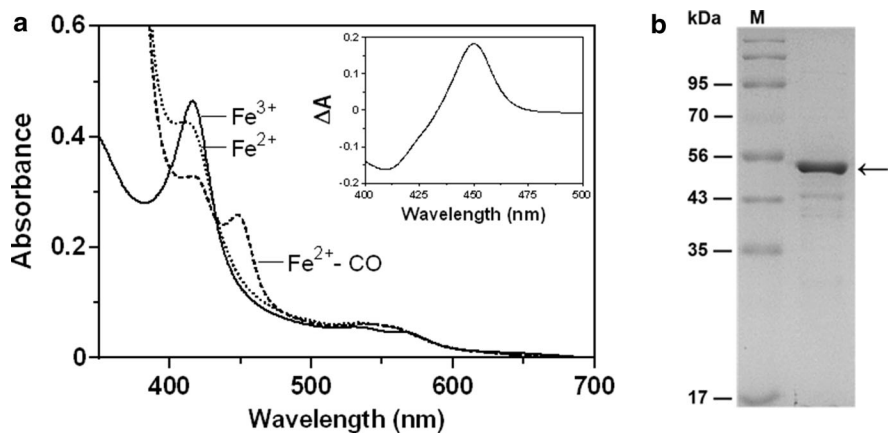

Fig. 1 Absorption spectra of purified CYP191A1 from *Mycobacterium smegmatis*. **a** The absorption spectra of the ferric, sodium dithionite-reduced ferrous, and ferrous-CO complexes of purified CYP191A1 in 100 mM potassium phosphate buffer (pH 7.4) are shown. The *inset* shows the reduced carbon monoxide difference spectrum of purified CYP191A1. **b** SDS-PAGE showing the standard molecular weight markers and the purified CYP191A1 enzymes

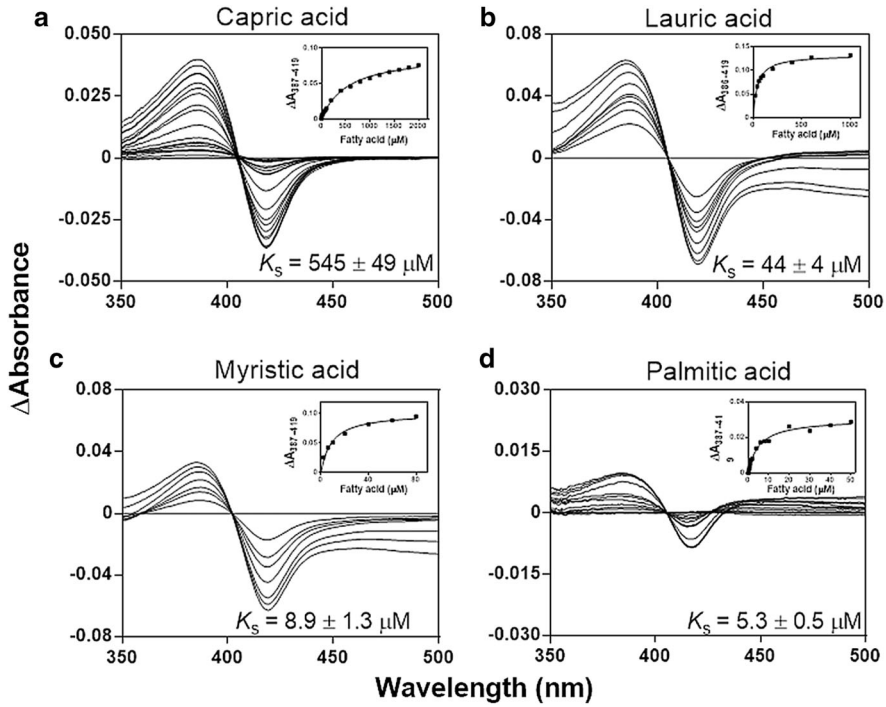

Fig. 2 Titration of ferric CYP191A1 with capric acid (**a**), lauric acid (**b**), myristic acid (**c**), and palmitic acid (**d**). The absorption spectrum of the ferric form (350–500 nm) was recorded following the addition of the fatty acids. The *inset* shows the changes in the absorbance, which were recorded using the dual wavelength mode, as a function of the indicated fatty acid concentration

the active site was unable to sufficiently alter the environment of the active site to result in spectral changes.

Catalytic activities of CYP191A1 toward fatty acids

The catalytic activities of the CYP191A1 toward fatty acids were investigated at a fixed substrate concentration (2 mM each fatty acid). The effects of the different electron transfer systems on the CYP191A1-catalyzed fatty acid hydroxylation were measured using a GC–MS analysis. None of the products were observed in the presence of the reductase systems used in this study, including rCPR, CaCPR, FDR/Fdx and PDR/Pdx, whereas CYP191A1 exhibited apparent activities for fatty acid hydroxylation at the ω-1 and ω-2 positions in the peroxide-supported reactions. In general, the *t*-BHP-supported reactions exhibited much higher activities than did the H_2O_2-supported reactions. For ω-1 hydroxylation supported by *t*-BHP, the CYP191A1 enzyme exhibited a higher activity for shorter fatty acids in the order $C_{10} > C_{12} > C_{14} > C_{16}$. For ω-2 hydroxylation, the enzyme preferred the medium-sized fatty acids C_{12} and C_{14} (Fig. 3). These results suggest that a proper position of the hydrocarbon within the active site is necessary for hydroxylation to occur.

The regioselectivity of each fatty acid was observed in the presence of H_2O_2 and *t*-BHP (Fig. 3). The CYP191A1 converted capric acid into the ω-1 and ω-2 monohydroxylated products in the presence of both peroxides. Specifically, capric acid is monohydroxylated in the ω-1, ω-2, and ω-3 positions with a regioselectivity of 89, 10, and 1%, respectively, in the presence of H_2O_2, and these values were comparable to the values of 93, 6, and 1% observed for the ω-1, ω-2, and ω-3 positions, respectively, in the case of *t*-BHP (Fig. 3a). Particularly, the rate of ω-1 monohydroxylation of CYP191A1 for capric acid in the presence of *t*-BHP was approximately sevenfold higher than those supported by H_2O_2, whereas the rate of ω-2 monohydroxylation of CYP191A1 supported by *t*-BHP was approximately fourfold higher than that observed in the presence of H_2O_2. Lauric acid is converted into ω-1 and ω-2 monohydrxylated products with a regioselectivity of 53 and 47%, respectively, in the presence of H_2O_2. The *t*-BHP-supported reaction also resulted in similar regioselectivity values (50:50 of ω-1 and ω-2 monohydroxylation) relative to that of the H_2O_2-supported reaction (Fig. 3b). The hydroxylation rate of CYP191A1 for lauric acid supported by *t*-BHP is

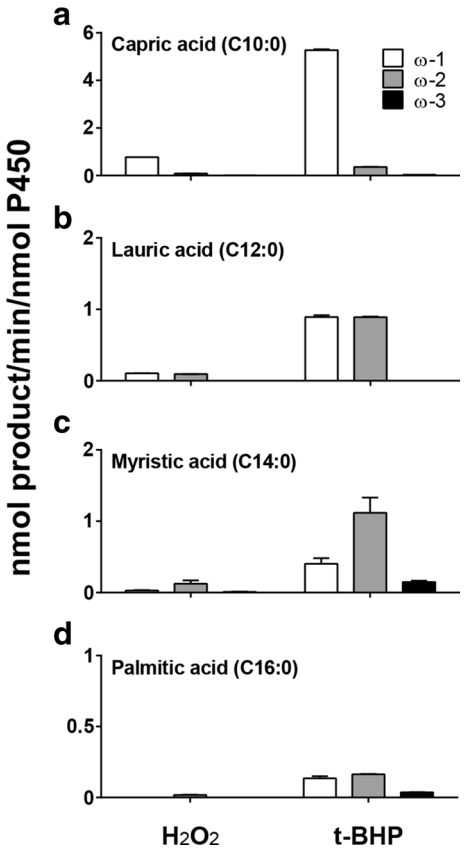

Fig. 3 Catalytic activities of CYP191A1 toward fatty acids. The hydroxylation of fatty acids at the ω-1, ω-2 and ω-3 positions by CYP191A1 were characterized; **a** capric acid; **b** lauric acid; **c** myristic acid; **d** palmitic acid. The oxidation rates of CYP191A1 in the presence of H_2O_2 and *t*-BHP were compared. The values are presented as the mean ± SD of triplicate determinations

approximately ninefold higher than that observed in the presence of H_2O_2.

CYP191A1 converted myristic acid into ω-1, ω-2, and ω-3 monohydroxylated products, with a regioselectivity of 18, 76, and 6%, respectively, in the presence of H_2O_2. In the case of the *t*-BHP-supported reaction, the regioselectivity was 24, 67, and 9% for ω-1, ω-2, and ω-3 hydroxylation, respectively (Fig. 3c). The hydroxylation rate of CYP191A1 for myristic acid in the presence of *t*-BHP was ~sevenfold higher than that in the presence of H_2O_2. Specifically, the rate of ω-1 hydroxylation in the presence of *t*-BHP was 14-fold higher than that observed in the presence of H_2O_2, and the rate of ω-2 hydroxylation in the presence of *t*-BHP was ninefold higher than that observed in the presence of H_2O_2. Moreover, the rate of ω-3 hydroxylation in the presence of *t*-BHP was 13-fold higher than that observed in the presence of H_2O_2. The oxidation rates of palmitic acid were much lower than those of C_{10}-C_{14} fatty acids, which were <0.3 min^{-1} (Fig. 3d). Palmitic acid is transformed by CYP191A1 into an ω-2 monohydroxylated product only in the presence of H_2O_2, whereas this substrate was hydroxylated at the ω-1, ω-2, and ω-3 positions with a regioselectivity of 40, 49 and 11%, respectively, in the presence of *t*-BHP (Fig. 3d).

Collectively, our results demonstrate that the CYP191A1 resulted in different regioselectivities at the ω-1, ω-2, and ω-3 positions depending on the specific fatty acid tested although information regarding the natural substrates of CYP191A1 is not currently available. The hydroxylation rates of CYP191A1 for fatty acids in the presence of *t*-BHP were higher than those observed in the presence of H_2O_2.

Catalytic activities of CYP191A1 toward chromogenic and fluorogenic substrates

Chromogenic and fluorogenic substrates are useful for catalytic activity assays. The assays can be used for HTS and continuous monitoring. The hydroxylation activity of the CYP191A1 toward 4-NP was measured at a fixed substrate concentration (800 μM) (Fig. 4a). To examine whether CYP191A1 can metabolize 4-NP, which is a typical human CYP2E1 substrate, via an electron transfer system, the metabolite 4-nitrocatechol was analyzed using a spectrophotometer. The CYP191A1 exhibited apparent catalytic activities in the presence of rCPR, PDR/Pdx, H_2O_2 and *t*-BHP in the range of 0.01–0.12 min^{-1} (Fig. 4a). In the presence of PDR/Pdx, the CYP191A1 exhibited the highest activity. However, the CaCPR and FDR/Fdx systems did not support the reaction.

The oxidation rates of CYP191A1 toward fluorogenic substrates, including 7-EC (Fig. 4b) and 7-EFC (Fig. 4c) were investigated. When the 7-EC oxidation was examined at a fixed substrate concentration (1 mM), two major products, 7-OH coumarin and 3-OH 7-EC, were produced. The metabolites were the same metabolites produced by human P450 s (Yun et al. 2005). The enzyme exhibited no catalytic activity toward 7-EC in the presence of rCPR, CaCPR, and PDR/Pdx, whereas the enzyme exhibited the highest catalytic activity for this substrate in the

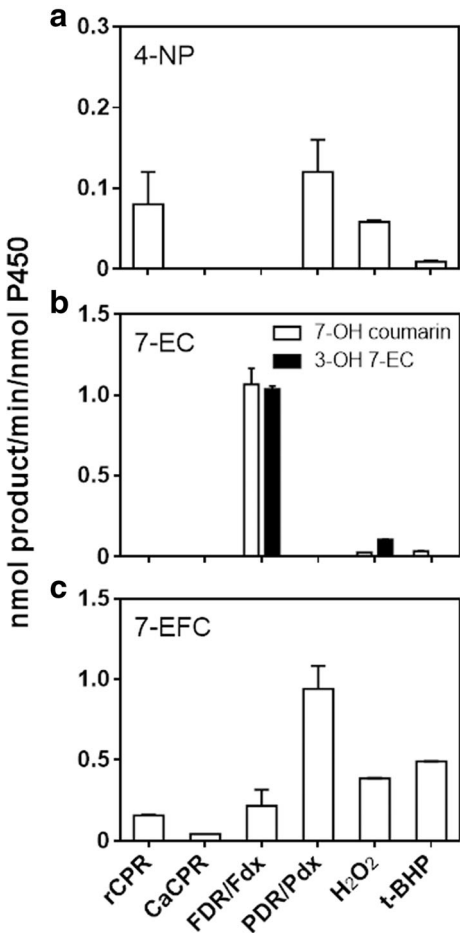

Fig. 4 Product formation of chromogenic and fluorogenic substrates by CYP191A1. The catalytic activities of CYP191A1 toward 4-NP in the presence of CPR, FDR/Fdx, PDR/Pdx, and peroxides (**a**) were examined. The catalytic activities of CYP191A1 for 7-EC (**b**) and 7-EFC (**c**) were analyzed using HPLC and spectrofluorometry, respectively. The values are presented as the mean ± SD of triplicate determinations

presence of FDR/Fdx. The FDR/Fdx system could support the oxidation activities of *O*-deethylation and 3-hydroxylation at a rate of up to 1.1 min^{-1}. The reaction in the presence of *t*-BHP and H_2O_2 proceeded at very low oxidation activities of 0.03–0.1 min^{-1}.

The catalytic activity of CYP191A1 was also investigated using 7-EFC, a substrate of several P450 s (Fig. 4c). A significant *O*-de-ethylation activity of CYP191A1 toward 7-EFC was observed in the presence of all electron transfer systems, including rCPR, CaCPR, FDR/Fdx, PDR/Pdx, H_2O_2 and t-BHP, with activities of 0.16 min^{-1}, 0.040 min^{-1}, 0.22 min^{-1}, 0.94 min^{-1}, 0.39 $min^{-1,}$ and 0.49 min^{-1}, respectively. Significantly, the activity in the presence of PDR/Pdx was the highest among all of the electron system tested here.

Catalytic activities of CYP191A1 toward human drug substrates

Simvastatin and lovastatin are oxidized by several human P450 s to produce at least four and three metabolites, respectively. CYP191A1 produced only two metabolites: one major (6′β-OH statin) metabolite and one minor (6′-exomethylene statin) metabolite, which are the same metabolites produced by the CYP102A1 mutant (Kim et al. 2011). The reactions in the presence of H_2O_2 were more active than those in the presence of *t*-BHP (Fig. 5a and b). Interestingly, simvastatin and lovastatin were the best substrates for the H_2O_2–supported CYP191A1 reactions among the set of substrates tested here. The distinct regioselectivity suggests that CYP191A1 prefers 6′β-OH product formation over 6′-exomethylene product formation. In the case atorvastatin, only hydrogen peroxide could support 4-hydroxylation reaction with values of 0.28 min^{-1} (Fig. 5c). When the hydroxylation reactions of simvastatin, lovastatin, and atorvastatin by CYP191A1 were performed in the presence of rCPR, CaCPR, FDR/Fdx, and PDR/Pdx, no apparent catalytic activities of the reactions were observed (<0.1 min^{-1}).

In addition, the ability of CYP191A1 to metabolize chlorzoxazone was measured at a fixed substrate concentration (200 μM chlorzoxazone). Chlorzoxazone, which is a typical human CYP2E1 substrate, was metabolized by CYP191A1 to yield 6-hydroxychlorzoxazone, which is also generated by human CYP2E1 (Peter et al. 1990). Although the hydroxylation reaction of chlorzoxazone was performed in the presence of rCPR, CaCPR, FDR/Fdx, PDR/Pdx, H_2O_2, and *t*-BHP, the catalytic activities of the reaction were identified only in the presence of peroxide (Fig. 5d). In the presence of both peroxides, the activities were similar to each other, with values of 0.2–0.21 min^{-1}. CYP191A1 showed very different results with respect to redox systems of rCPR and PDR/Pdx to two classic CYP2E1 substrates, 4-NP (Fig. 4a) and chlorzoxazone (Fig. 5d). Although both peroxides, H_2O_2 and *t*-HBP, hydroxylated both substrates, only rCPR and PDR/Pdx among four reductase systems could support the 4-NP hydroxylation but not

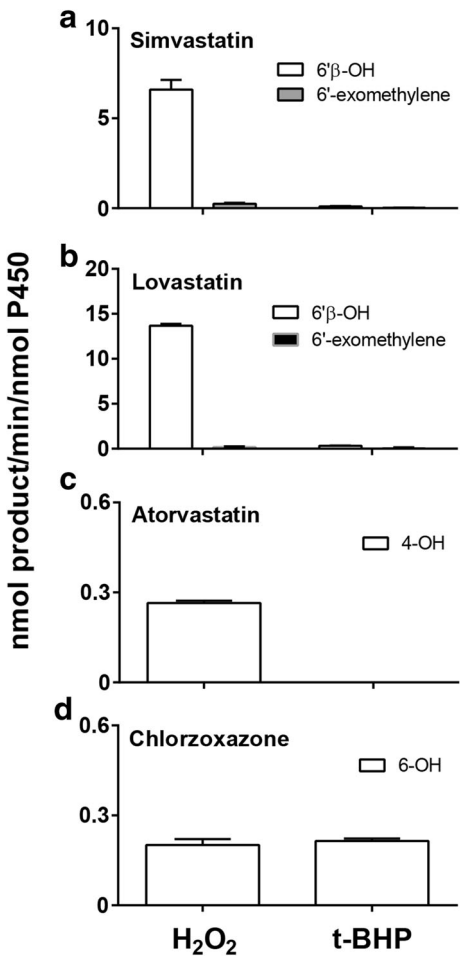

Fig. 5 Rates of product formation of human drug substrates by CYP191A1 in the presence of peroxides. In the case of statins, CYP191A1 produced two metabolites, 6′β-OH and 6′-exomethylene products, in the presence of H_2O_2 (**a**) and *t*-BHP (**b**). The rates of product formation of atorvastatin (**c**) chlorzoxazone (**d**) by CYP191A1 in the presence of peroxides were also evaluated. The values are presented as the mean ± SD of triplicate determinations

chlorzoxazone hydroxylation. This difference may result from distinctive effects of the substrates on the efficiency of electron transfer from reductase system to the P450.

CYP191A1 did not show apparent oxidation activity (<0.02 min^{-1}) toward phenacetin (1 mM), 7-ethoxyresorufin (5 μM), 7-methoxyresorufin(5 μM), 7-pentoxyresorufin (5 μM), coumarin (1 mM), and resveratrol (200 μM), which are typical substrates of human P450s (results not shown).

Despite the importance and usefulness of eukaryotic P450s, the low activity and structural instability of these enzymes limit their use as biocatalysts in several fields of industrial application (Julsing et al. 2008). To overcome these limitations, bacterial P450 s have been suggested as ideal alternatives to help understand the biocatalytic properties of these biocatalysts. Recently, research in the biotechnological fields has focused on the design and development of bacterial P450 enzymes for the production of pharmaceuticals and human drug metabolites (Urlacher and Girhard 2012). Interestingly, a large set of CYP102A1 variants have human P450-like activities and produce human metabolites of drugs (Whitehouse et al. 2012). Furthermore, the requirement of expensive cofactor NADPH and the reductase partner has limited the employment of P450s in the industry (Behrendorff, et al. 2015). The use of peroxide-supported P450 reactions should be cost-effective in the generation of human drug metabolites (Shoji and Watanabe 2014).

In summary

CYP191A1 catalyzes the same reaction that the human P450 enzymes catalyze to generate human metabolites (Supplementary Table 1). The similarities of the oxidation reactions between CYP191A1 and human P450s suggest a possible application of CYP191A1 as a model system for studying the human enzymes. In addition, the catalytic activities of CYP191A1 that were obtained using peroxides were higher than those obtained using other electron transfer systems. These results suggest that CYP191A1 can be developed as a biocatalyst to obtain human drug metabolites in a cost effective manner. Furthermore an extensive study for the 'natural' P450 electron transfer chain is necessary to determine the natural function of CYP191A1. The natural function of CYP191A1, however, remains unknown.

Acknowledgements This research was supported by the National Research Foundation of Korea (Grant NRF-2016R1A2B4006978), Republic of Korea.

Supporting information Supplementary Methods—Preparation of reductase systems.

Supplementary Methods—Construction of an expression plasmid for the CYP191A1 gene.

Supplementary Methods—Heterologous expression and purification of recombinant CYP191A1.

Supplementary Methods—CYP191A1 catalytic activity assays.

Supplementary Methods—Spectroscopy.

Supplementary Table 1—Comparison of the activities of CYP191A1-catalyzed oxidations to the marker activities of human P450 isoforms.

Supplementary Fig. 1—Chemical structures of substrates for CYP191A1 used in this study.

Supplementary Fig. 2—Amino acid sequence alignment of four P450 s of CYP191A subfamily from *Mycobacterium* genus.

References

Behrendorff JB, Huang W, Gillam EM (2015) Directed evolution of cytochrome P450 enzymes for biocatalysis: exploiting the catalytic versatility of enzymes with relaxed substrate specificity. Biochem J 467:1–15

Bernhardt R, Urlacher VB (2014) Cytochromes P450 as promising catalysts for biotechnological application: chances and limitations. Appl Microbiol Biotechnol 98:6185–6203

Frank DJ, Waddling CA, La M, Ortiz de Montellano PR (2015) Cytochrome P450 125A4, the third cholesterol C-26 hydroxylase from *Mycobacterium smegmatis*. Biochemistry 54:6909–6916

García-Fernández E, Frank DJ, Galán B, Kells PM, Podust LM, García JL, Ortiz de Montellano PR (2013) A highly conserved mycobacterial cholesterol catabolic pathway. Environ Microbiol 15:2342–2359

Guardiola-Diaz HM, Foster LA, Mushrush D, Vaz ADN (2001) Azole-antifungal binding to a novel cytochrome P450 from *Mycobacterium tuberculosis*: implications for treatment of tuberculosis. Biochem Pharmacol 61:1463–1470

Jackson CJ, Lamb DC, Marczylo TH, Parker JE, Manning NL, Kelly DE, Kelly SL (2003) Conservation and cloning of CYP51: a sterol 14 alpha-demethylase from *Mycobacterium smegmatis*. Biochem Biophys Res Commun 301:558–563

Julsing MK, Cornelissen S, Buhler B, Schmid A (2008) Heme-iron oxygenases: powerful industrial biocatalysts? Curr Opin Chem Biol 12:177–186

Kim KH et al (2011) Generation of human chiral metabolites of simvastatin and lovastatin by bacterial CYP102A1 mutants. Drug Metab Dispos 39:140–150

Ouellet H, Johnston JB, Ortiz de Montellano PR (2010) The *Mycobacterium tuberculosis* cytochrome P450 system. Arch Biochem Biophys 493:82–95

Peter R, Böcker R, Beaune PH, Iwasaki M, Guengerich FP, Yang CS (1990) Hydroxylation of chlorzoxazone as a specific probe for human liver cytochrome P-450IIE1. Chem Res Toxicol 3:566–573

Poupin P, Ducrocq V, Hallier-Soulier S, Truffaut N (1999) Cloning and characterization of the genes encoding a cytochrome P450 (PipA) involved in piperidine and pyrrolidine utilization and its regulatory protein (PipR) in *Mycobacterium smegmatis* mc2155. J Bacteriol 181: 3419–3426

Shoji O, Watanabe Y (2014) Peroxygenase reactions catalyzed by cytochromes P450. J Biol Inorg Chem 19:529–539

Urlacher VB, Girhard M (2012) Cytochrome P450 monooxygenases: an update on perspectives for synthetic application. Trends Biotechnol 30:26–36

Warrilow AG, Jackson CJ, Parker JE, Marczylo TH, Kelly DE, Lamb DC, Kelly SL (2009) Identification, characterization, and azole-binding properties of *Mycobacterium smegmatis* CYP164A2, a homolog of ML2088, the sole cytochrome P450 gene of *Mycobacterium leprae*. Antimicrob Agents Chemother 53:1157–1164

Whitehouse CJ, Bell SG, Wong LL (2012) P450(BM3) (CYP102A1): connecting the dots. Chem Soc Rev 41:1218–1260

Yun CH, Kim KH, Calcutt MW, Guengerich FP (2005) Kinetic analysis of oxidation of coumarins by human cytochrome P450 2A6. J Biol Chem 280:12279–12291